CHAPTER THREE

On Multiple Falls, End Point Height and Sound Phenomena

The deceleration during a relatively direct atmospheric penetration is found to rise to a maximum value and then decrease during descent. The maximum value can be shown to occur when the velocity has been reduced to $e^{-1/2}$ or about 61% of its initial value. The maximum deceleration is

$$\left(\frac{dv}{dt}\right)_{max} = -\frac{av^2 \sin\phi}{2e}$$

It is interesting to note that the size of the maximum deceleration is independent of the drag/mass characteristics of the body. It is dependent only upon the path angle, the initial velocity and the atmospheric characteristics. However, the *altitude* at which the maximum deceleration occurs is dependent upon the drag/mass characteristics.

The effect of entry angle is illustrated in Table 9 for an average iron meteorite of 25 kg, with an initial velocity of 20 km/sec and a radius of 9.12 cm.

Table 9. The Deceleration is Strongly Dependent Upon the Approach Angle

Approach Angle	K	Maximum deceleration km/sec²	Equivalent g*
90°	0.0053	10.50	1070
53°.9	0.0065	8.50	865
4°.6	0.065	0.85	87

*Standard acceleration of gravity g = 9.80665 m/sec²

The smaller entry angle is seen to result in deceleration higher in the atmosphere (larger K values) and in significantly smaller peak decelerations.

An examination of Table 10 and Figure 15 shows that of 32 well-observed falls, nine are known positively to have burst in the atmosphere, subjected to these violent decelerations. For at least six of the others, eyewitness reports and examinations of the recovered masses indicate that several fragments were produced in the atmosphere, while only one was recovered. As will be noted repeatedly in the later individual descriptions of iron meteorites, these are far from being massive, high strength bodies when they arrive at our atmosphere. On the contrary it may be assumed that the irons (i) possess several grain boundary cracks, (ii) contain low strength, partly fissured minerals, such as troilite, schreibersite and, to a minor degree, cohenite, graphite, chromite and silicates, and (iii) contain microcracks in the cubic kamacite phase. The majority of these fissures and damages are presumably due to previous cosmic collisions. Additional fissures are probably created during the atmospheric flight.

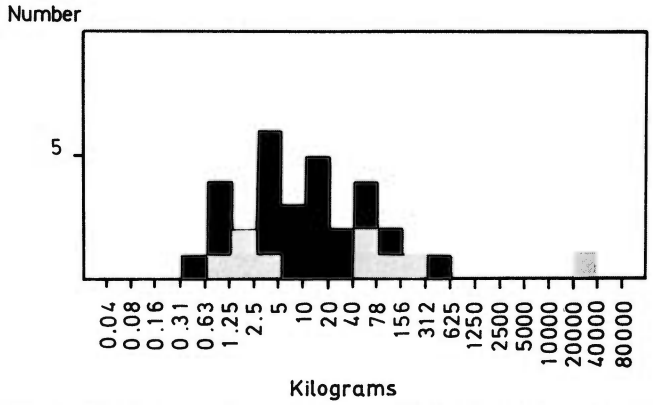

Figure 15. A histogram of the best documented falls. A gray square indicates a multiple fall, while black indicates the total number of falls within a given mass range.

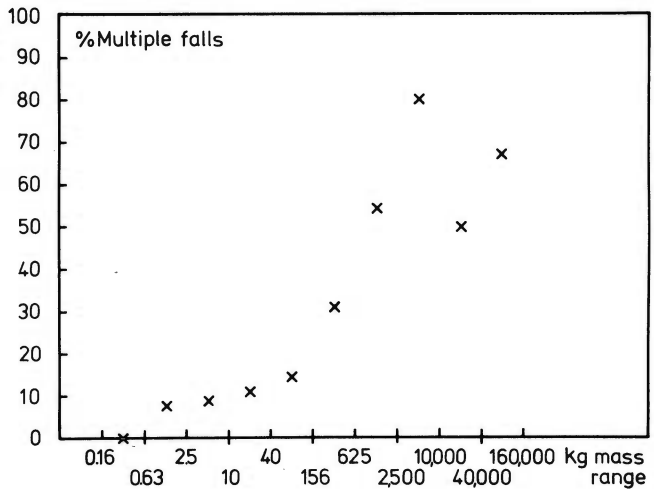

Figure 16. The frequency of multiple falls increases monotonically with increasing initial mass.

The statistics including *all* finds and falls are less accurate but show the same general trend, Table 12. Figure 12 is based upon 495 iron meteorites; i.e., all the well-substantiated finds and falls treated in this manual. Of these, no less than 78 are known to have produced multiple falls giving rise to two or, often, more fragments.

Figure 16 shows that the frequency of multiple falls increases monotonically as the size of the meteorite

increases. If one large meteorite is discovered the probability is over 50% that additional fragments should be found in the vicinity. On the other hand, irons smaller than 100 kg will have a good chance of surviving the atmospheric flight as entire bodies. The common belief that iron meteorites possess sufficient strength to travel through the atmosphere without fragmentation thus needs qualification.

In Table 11 data for important iron meteorite showers, comprising six or more individuals have been collected. Meteorite showers are usually spread over a narrow elliptical area, called a dispersion ellipse. Many stone meteorites have produced showers with well-mapped dispersion ellipses, such as Bruderheim, Homestead, Kunashak and Allende, the last mentioned resulting in two tons of fragments within a 50 X 100 km ellipse (Clarke et al. 1971a). The individual specimens usually show a characteristic distribution within the dispersion ellipse. The larger pieces travel farthest and are found at the far end of the ellipse, relative to the direction of travel, while the smallest pieces are found in the opposite part (Figures 17 and 18).

The characteristics are not well known for iron meteorites because so few showering falls have been observed. Table 20 and Figure 1624 illustrate the well mapped Sikhote-Alin case, covering an area of 2.0 X 0.8 km, with the largest masses producing impact holes at the southern end. The meteorite had approached from N 15° E with an initial inclination, ϕ, of 41° (page 1123). Other showers have scattered debris over much larger areas, most notably Gibeon, Figure 780, of which fragments have been found within an elliptical area of 250 X 100 km.

Table 10. Iron Meteorite Falls. 32 are listed, but not all are equally well documented

	Class	Group	% Ni	Fell Year	Fell Day	Fell Month	Fell Local time	Total kg	Total No.	Largest mass, kg.	Smallest mass, kg.	Main mass in
Hraschina, Yugoslavia	Om	IID	10.6	1751	26	May	18:00	48.7	2	39.7	9	Vienna
Charlotte, U.S.A.	Of	IVA	8.3	1835	1	Aug.	14:30 ?	4.0	1	4.0	–	Harvard
Braunau, Czechoslovakia	H	IIA	5.4	1847	14	July	03:45	40.8	2	23.6	17.2	Prague
Nedagolla, India	Anom	Anom	6.1	1870	23	Jan.	19:00	4.6	1	4.6	–	London
Rowton, England	Om	IIIA	7.8	1876	20	April	15:40	3.5	1	3.5	–	London
Mazapil, Mexico	Om	I	8.5	1885	27	Nov.	21:00	3.95	1	3.95	–	Vienna
Hassi-Jekna, Algeria	Of	IIIC	10.5	1885	–	–	–	1.25	1	1.25	–	Paris
Cabin Creek, U.S.A.	Om	?	?	1886	27	March	15:17	48	1	48	–	Vienna
Quesa, Spain	Om	?	?	1898	1	Aug.	20:45	10.7	1*	10.7	–	Vienna
Magnesia, Turkey	Om	IIIC	11.0	1899		unknown		> 5	1*	5	–	Paris
N'Goureyma, Mali	Anom	Anom	9.4	1900	15	June	?	37.7	1	37.7	–	Heidelberg
Okano, Japan	H	IIA	5.4	1904	7	April	06:35	4.7	1	4.7	–	Kyoto
Avče, Yugoslavia	H	IIA	5.5	1908	31	March	08:45	1.23	1	1.23	–	Vienna
N'Kandhla, South Africa	Om	IID	10.0	1912	1	Aug.	13:30	17.5	1	17.5	–	London
Annaheim, Canada	Og	I	7.8	1914	21	Jan.	14:30	13.8	1	13.8	–	Ottawa
Treysa, Germany	Om	IIB	9.5	1916	3	April	15:25	63.3	1	63.3	–	Marburg
Boguslavka, Siberia	H	IIA	5.4	1916	18	Oct.	11:47	257	2	199	58	Moscow
Garhi Yasin, Pakistan	Om	Anom	8.3	1917		Jan., night time ?		0.38	1*	0.38	–	London
Norfork, U.S.A.	Om	IIIA	7.9	1918		Oct., night time ?		1 ?	?	?	?	Tempe
Rembang, Indonesia	O	IVA	8.7	1919	30	Aug. ?		10	1	10	–	Djakarta ?
Pitts, U.S.A.	Of	Anom	12.9	1921	20	April	09:00	3.8	4	1.6	0.05	Washington
Samelia, India	Om	IIIA	8.0	1921	20	May	17:30	2.5	3	1.13	0.58	Calcutta
Udei Station, Nigeria	Om	I-An	8.9	1927		Jan.-Mar., daytime		103	1*	103	–	Kaduna
Repeev Khutor, Russia	Opl	Anom	14.3	1933	8	Aug.	22:00	12.35	1*	12.35	–	Moscow
Bahjoi, India	Og	I	7.7	1934	23	July	21:30	10.3	1*	10.3	–	Calcutta
Nyaung, Burma	?	?	?	1939	24	Dec.	19:40	0.7	1	0.7	–	Calcutta
Scroti, Uganda	Anom	Anom	12.9	1945	17	Sept.	13:10	2.0	5	1.00	0.17	Entebbe
Sikhote-Alin, RSFSR	Ogg	IIB	5.9	1947	12	Feb.	10:38	23,000	> 400	1745	~ 0.001	Moscow
Yardymly, Azerbaidjan	Og	I	6.8	1959	24	Nov.	07:05	153	6	127	0.36	Baku
Bogou, Upper Volta	Og	I	7.1	1962	14	Aug.	10:00	8.8	1*	8.8	–	Upper Volta
Muzzaffarpur, India	Opl	Anom	12.9	1964	11	April	17:00	1.24	2	1.09	0.15	Calcutta
Juromenha, Portugal	D	IIIAB	8.7	1968	14	Nov.	17:55	25.2	1	25.2	–	Lisbon

Asterisks indicate that more than one mass fell but that only one was recovered.

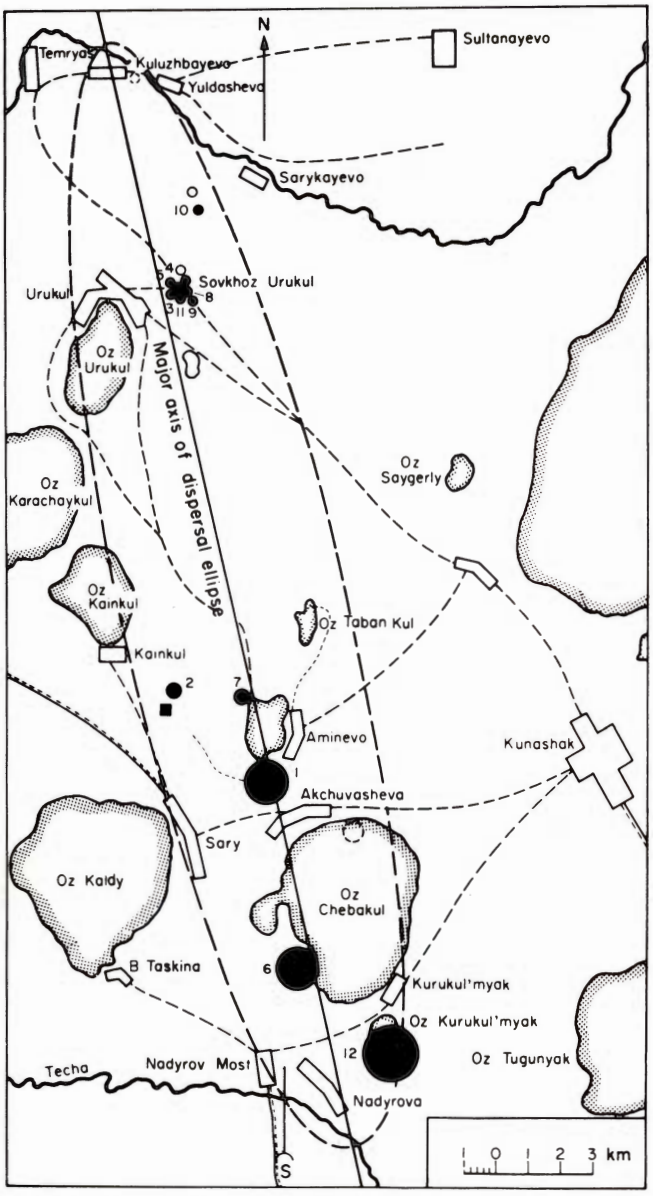

Figure 17. Distribution ellipse of the Kunashak stone meteorite (L6) shower that fell near Sverdlovsk, USSR, in 1949. Twenty specimens totaling over 200 kg were found; their relative sizes are indicated with the rings. (From Krinov 1966a.)

However, this seems to be an extreme and very unusual case. A more normal case is treated under Tombigbee (page 1218 and Figures 1769-1778).

An analysis of iron meteorite data, Table 12, for all 495 finds and falls allows the following conclusions to be drawn:

(i) Seventy-eight, or on the average 16%, fragmented in flight. It appears that the percentage of multiple falls increases smoothly with the initial mass.

(ii) The curve showing multiple falls vs. (final) mass, Figure 16, breaks at a point about the 100 kg mass. Below this, only about 10% suffer fragmentation, and above it on the average about 50%.

(iii) The total quantity of recovered iron meteorites in the world is about 460,000 kg or 460 tons. Of this, 90% comes from the 20 largest meteorites. Only one of these, Sikhote-Alin, is an observed fall.

Figure 18. Thirty-eight of the 230 stones collected within a 20 x 5 km dispersion ellipse after the Tenham (L6) fall in Queensland, 1879. Scale bar is 10 cm. (From Hodge-Smith 1939.)

(iv) The large iron meteorites that survived fragmentation, Hoba, Armanty, Bacubirito, Mbosi, Willamette and Morito, are, as far as we know, – for they have not been subjected to very much cutting – rather inclusion-free; if schreibersite and carbides do occur, they are in the form of minute evenly dispersed particles. As the absolute contrast we may note the frequent and large troilite and schreibersite inclusions of Canyon Diablo, Cape York, Campo del Cielo, Chupaderos, Sikhote-Alin, Mundrabilla and Cranbourne, all of which produced extensive showers. Gibeon is an exception. Its pure and homogeneous metal phase with scattered troilite inclusions would hardly be expected to yield such an extensive shower as recorded. It appears that Gibeon must have had very unusual flight characteristics.

(v) Figure 19 indicates that the number of meteorites within each size range decreases smoothly. The most common size of an iron meteorite is 10-20 kg. Below this mass range, the curve shows an abrupt break and small meteorites become increasingly rarer. The explanation for the break is apparently duplex: small meteorites are difficult to find, but if found, they tend to remain in

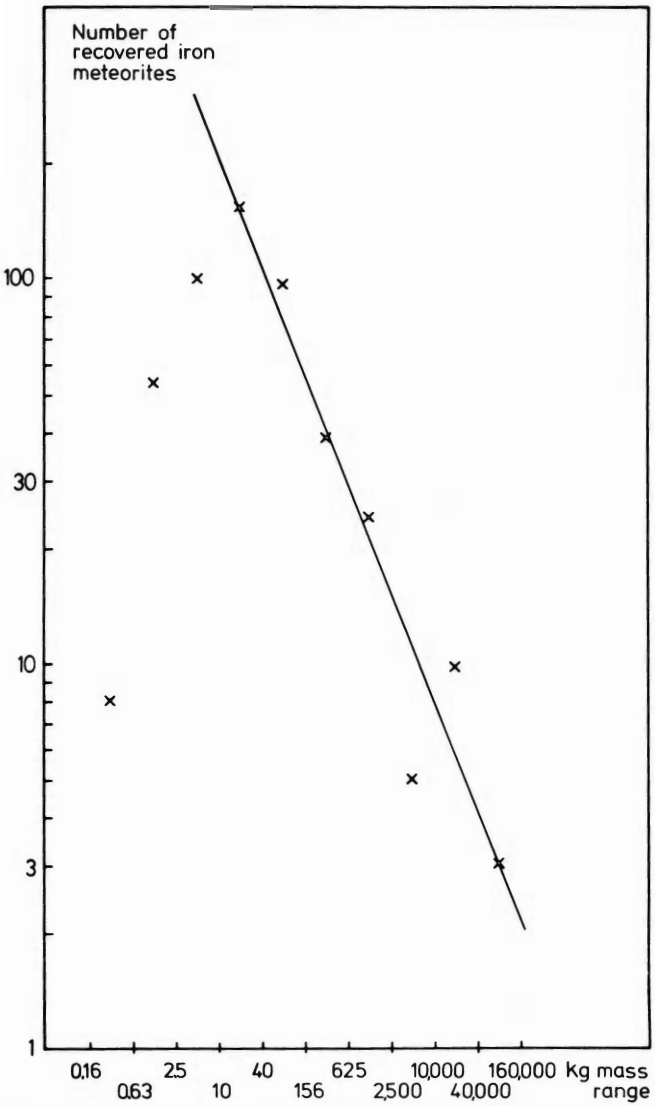

Figure 19. The number of recovered iron meteorites versus size. Data from Table 12.

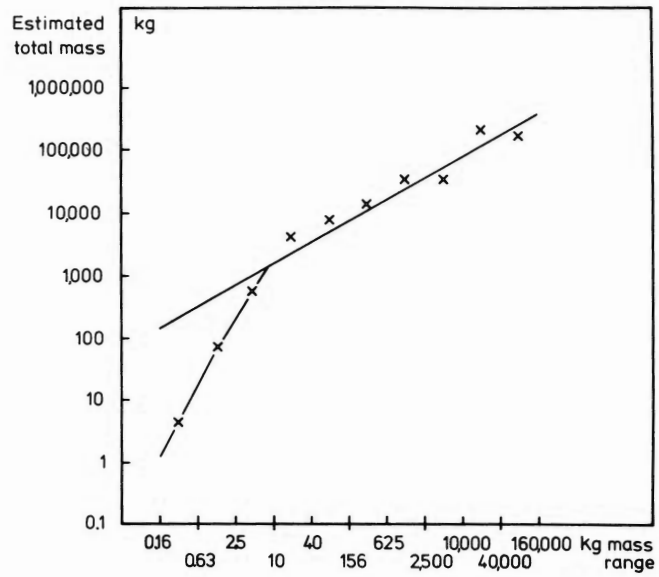

Figure 20. The total mass of recovered iron meteorites within each mass range. Data from Table 12.

private possession or to become converted into some kind of implement, etc., as is repeatedly shown in this manual. They are thus lost to science if ever found.

Figure 20 may be interpreted in a similar way although the data vary widely. An alternative but less plausible explanation of Figures 19 and 20 would be to take the numbers at face value and conclude that small iron meteorites are relatively rare at Earth's distance from the Sun.

The End Point Height and the Dark Part of the Trajectory

The maximum deceleration of fireballs and meteorites usually takes place in the zone between an altitude of 50

Table 11. Selected Important Showers

	Class	Group	% Ni	Found	Total kg	Total No.	Long axis of the dispersion ellipse, km	Three largest masses kg 1	2	3	Two smallest masses kg 4	5
Youndegin	Og	I	6.7	1844	3800	13	25	2626	927	173	0.82	0.42
Toluca	Og	I	8.1	1784	> 3000	> 2000	5	400	150	107	0.1	0.05
Coahuila	H	IIA	5.6	1854	> 2000	> 20	2 ?	318	250	250	4.5	1.0
Magura	Og	I	6.7	1840	> 1800	> 100	3 ?	42	10.5	5.0	0.5	0.2
Santa Rosa	Anom	Anom	6.7	1810	825	9	15	612	100	41	0.68	0.56
Arispe	Og	Anom	6.7	1898	683	17	20	124	122	69.8	9.0	9.0
Trenton	Om	IIIA	8.3	1868	506	13	0.4	239	187	28.1	1.35	0.70
Morasko	Og	I	6.7	1914	300	> 25	1.4	78	77.5	75	2	1
North Chile	H	IIA	5.6	1922	266	8	< 60	78	74	29	19	4.2
Glorieta Mt.	Pall	Anom	11.9	1884	190	28	4	67.4	52.4	24.3	0.17	0.13
Yardymly	Og	I	6.8	F:1959	153	6	8	127	11.3	5.9	2.3	0.36
Chinga	D	IVB	16.5	1912	80	30	1 ?	20.5	9.7	3.8	0.29	0.09
Smithville	Og	I	6.9	1840	72	11	1	29.5	16.3	6.8	1.3	0.50
Tombigbee	H	Anom	5.1	1859	44	6	14	15.0	12.0	9.2	3.26	0.76
Deport	Og	I	8.2	1926	> 15	26	1 ?	5.8	2.8	1.3	0.3	0.2

Other showers: See Tables 18 and 20, and Bingera.

and 10 km. As a result the initial velocity, v_∞, averaging 17 km/sec, will be reduced to perhaps 3 km/sec, and the trail will cease to be luminous because too small an energy is dispersed for ionization of the air The body itself will from now on be effectively cooled by a forced airdraft. The point of the trajectory where the fireball disappears to the observer, i.e. where the luminous trail ends, has been called the end point, the zone of retardation, and in German, *Hemmungspunkt*. Its altitude is relatively well observed for a number of fireballs and meteorites, as may be seen from Table 13. The meteorite velocity at the end point is, however, very inaccurately known but may be estimated to be of the order of 3-6 km/sec. A recent determination by multiple-station photography yielded an end point velocity of 3.5 km/sec for the largest 10 kg fragment of the Lost City shower (McCrosky et al. 1971). In Table 13 some data are also given for the angle, Φ, between the trajectory and the horizontal, the initial velocity, and the estimated altitude where the fireball was first observed. This altitude is, however, very uncertain, except when based upon photography. A good discussion of the end point height is to be found in McIntosh (1970).

The height of the end point ranges from 5 to 64 km. The highest observed end point for a meteorite-producing fireball is 42 km (Pultusk), but the end points for most meteorites lie below 30 km, and – from more detailed material not presented here – may be estimated to average 18 km. There is an indication, however, that all observed iron meteorites have left luminous trails to lower altitudes than 18 km. This is probably caused by their relatively

Table 12. Analysis of the Number of Iron Meteorites in Various Mass Ranges, and the Frequency of Multiple Falls

Mass range kg	Total number	Estimated total mass kg	Multiple falls	
			number	%
0.16-0.63	8	3.5	0	0
0.63-2.5	53	84	4	7.5
2.5-10	101	580	8	8.0
10-40	155	3,350	16	10.3
40-156	97	8,000	14	14.4
156-625	39	13,000	12	30.8
625-2,500	24	31,000	13	54
2,500-10,000	5	30,000	4	80
10,000-40,000	10	212,000	5	50
40,000-160,000	3	160,000	2	67
Grand total	495	458,000	78	16

Table 13. End Point Heights and Lengths of Typical Trajectories

Name	Type*	Φ	Velocity km/sec		Height, km		Length of trajectory	Recovered mass kg
			initial V_∞	end point V	first observed	end point		
Sikhote-Alin	I	41°	14.5		–	5	–	23,000
Paragould	S	14°	19		45	8	153	405
Zhovtnevyi	S	43°	18		124	8	158	107
Přibram	S	43°	20.9	~ 7	98	13.3	124	9.5
Braunau	I					15 ?		41
Treysa	I	55°	> 20		83	16	81	63
Pasamonte	S	12°	20		141	17	670	4
Lost City	S		14.2	3.5	86	19.5		17
Orgueil	S	18°			280 ?	22	721	~ 10
Bjurböle	S	24°			135	24	329	330
Bruderheim	S	40°	15		48	26	40	303
40617, Prairie Netw.	F		13.2	4.2	80	26		
Aarhus	S	20°	15		143	31	304	0.7
New York-Quebec	F	4°	17.0		67	33	500	–
1242, Harvard	M	51°	12.2	8.1	75	37	60	–
27471, Ondrejov	M		26.0	13.2	87	41		–
Pultusk	S	44°			178 ?	42	186	~ 250
19816, New Mexico	M	44°	20.7	9.2	91	47	62	–
1.11.1956, Alberta	M		13.0		69	64	~ 7	–

*S, stone meteorite; I, iron meteorite; F, fireball; M, meteor.

good coherence which secures an almost constant low K-value during most of the trajectory. Stones, on the contrary, may fragment early, and each of the resultant masses will have higher K-values than the initial body and thus suffer deceleration at a higher altitude than if the whole mass persisted as an entity. Finally, a small contribution to the light from a falling iron meteorite may come from exothermic burning of the metal to oxides during the latter part of the trajectory in the dense atmosphere.

After the major deceleration has occurred, the meteorite trajectory bends over into a vertical descent, and the velocity is essentially a local terminal fall velocity only governed by gravity and air resistance. For the free fall *in vacuum* we have $s = \frac{1}{2}gt^2$; $v = gt$; $g = dv/dt$. The terminal velocity in vacuum, v_v, is given in Table 14, for different altitudes of start:

Table 14. Terminal Velocities v_v in Vacuum

Start at	v_v	Start at	v_v
100 km	1410 m/sec	10 km	450 m/sec
40 km	890 m/sec	5 km	310 m/sec
20 km	630 m/sec	1 km	141 m/sec

In air the terminal velocity v_t is dependent on the mass and the drag coefficient. The following values have been obtained from experiments with small bombs (Astapovich 1958: 500):

Table 15. Terminal Velocities v_t in Air

Mass in kg	8	16	30	74	164
v_t in m/sec	151	162	192	231	276

The terminal velocity v_t is, in practice, reached after a few seconds. Several visual observations of small meteorite falls indicate that the terminal fall for masses of 1 to 100 kg occurs vertically with velocities of 125-250 m/sec. In Hessle, near Uppsala, Sweden, a large shower of stones fell on New Year's Day 1869, and samples were recovered from the surface of frozen lakes. It was evident that masses of about 1 kg had not been able to penetrate ice of one or two inches in thickness. The 794 g Beddgelert stone meteorite which fell on September 21, 1949, penetrated the roof of a hotel. It made a neat round hole in four overlapping thicknesses of slate, about 17 mm thick, and broke through the plaster ceiling into the room below where it came to rest on the floor (Chackett et al. 1950).

Small stone meteorites may display a surprisingly gentle fall. Many individual fragments, of 25-100 grams, from the Allende shower were thus picked up with delicate surface features, such as filamentary fusion crusts, which had not been damaged upon hitting the ground. Other, larger fragments from the same shower, however, displayed spalled fusion crusts and freshly broken corners; more severe fragmentation occurred in some cases where kilogram-sized Allende fragments hit the ground.

Iron meteorites of average size (10-20 kg) will survive intact when hitting the surface of the ground, except in such cases where serious cracks were already created during the deceleration in the atmosphere. The metallic matrix of iron meteorites is usually so ductile that an early fracture – from aeons-old cosmic collisions or from atmospheric deceleration – does not necessarily lead to full separation upon impact with the ground. Such deep cracks which almost divide the iron meteorites into two fragments are, for example, present in Descubridora, Hoba, Monohans, Lazarev and some Sikhote-Alin specimens. Other Sikhote-Alin masses split partially in the atmosphere and then finally broke up when penetrating the frozen earth. In many impact holes a number of fragments were thus found close together; they clearly showed both atmospheric external fractures and late internal fractures, and fragments from the same hole could easily be fitted together to an entire mass, see page 1123.

The wind effect is pronounced during the dark-flight trajectory through the troposphere. Aloft, wind speeds are usually much greater than those registered near the ground; see Figure 13. In general, the wind increases with height up to near the tropopause (~ 12 km), and the strongest winds easily attain velocities of 50 m/sec. The so-called jet streams exceed 100 m/sec. In all of the recent and well studied stone meteorite falls, Příbram, Allende and Lost City, significant deviations from the predicted points of impact have occurred due to the prevailing winds in the troposphere. A 10 kg fragment of Lost City was thus carried 4 km eastwards relative to the impact point predicted from the ballistic flight data alone (McCrosky et al. 1971).

Heating and Ablation

The reduction of the meteorite's kinetic and potential energy during descent is accompanied by an increase in thermal energy in the surrounding air, some of which is transferred to the meteorite surface. This fraction depends upon the shape, velocity and altitude of the meteorite, and ultimately on the mechanism of heat transfer between the hot gas and the meteorite. At very high altitudes, in the free molecule flow region, where the heat energy is developed directly at the meteorite's surface, as much as one half of the meteorite's lost energy can appear as heat in the body. At lower altitudes, in the continuous flow region, thermal energy appears in the air between the shock wave front and the body. Heat is transferred from this hot air to the body by conduction and convection through a viscous boundary air layer; radiation from the hot gas will also contribute considerably to the surface heating. The heat goes to increase the surface temperature of the meteorite which may be assumed to be 273° K (0° C) when coming in from space. As the surface melts, vaporizes and ionizes, a heat front penetrates into the interior of the mass. The ablated, vaporized material tends to block the flow of heat from the hot shock layer into the body. The ablated, melted material may be swept away from the body as streamers of molten

metal that oxidize in the air (if enough oxygen is present) and solidify to tiny droplets, 1-100 μ in diameter, that precipitate as meteoritic dust. A minor part of the molten material may stream to the rear side of the meteorite and be redeposited as laminated, dendritic material. The total process is thus extremely complicated, although everything happens within a few seconds. The process may be roughly compared to heating a massive, cold iron lump intensively with oxygen-acetylene torches for a few seconds, and then changing over to a forced cooling with jet air streams. The meteorite is cold when it hits the ground, or indeed not warmer than it can be carried by hand.

The kinetic energy is $E = \frac{1}{2} m v^2$. The energy converted to heat per unit time is

$$\frac{dE}{dt} = m \cdot \dot{v} \cdot \frac{dv}{dt} = m \cdot v \cdot \frac{DA}{m} \rho \cdot v^2 = D \cdot A \cdot \rho \cdot v^3$$

The maximum heating rate can be shown to occur when the velocity has been reduced to about 80% of the initial velocity. The peak heating rate, therefore, occurs before the maximum deceleration load.

The portion of the heat reaching the body is normally a small fraction of the total energy; if it were not so, no meteorites would ever survive the atmospheric penetration. The actual calculation of the partition of heat between the flying body and the surrounding atmosphere is beset by many unknowns. The kinetic energy is converted into (i) heating of the body, (ii) surface melting, (iii) vaporization and ionization of metal vapor and air atoms, (iv) heating and translating the air mass in front of the meteorite, (v) formation of shock waves, (vi) rotation of the meteorite, and (vii) fragmentation of the meteorite. It is beyond the scope of this treatise to cover these phenomena in greater detail. The reader is referred to the papers by Öpik (1958b), Maringer & Manning (1960), Buchwald (1961b), Ceplecha (1961), McIntosh (1970), McCrosky et al. (1971) and Blanchard (1972) and also to the works mentioned on page 20.

The results of these studies indicate that, in general, 1-4 mm is lost per second of the flight. The ablational loss is probably confined to the part of the trajectory which is luminous. The lengths of the luminous trajectories range from about 40 km (Bruderheim) to about 700 km (Orgueil, Pasamonte). With an estimated average velocity, v_0, of about 10 km/sec, the meteorites may thus roughly become exposed to ablation for periods of four seconds to over one minute. The total amount of material lost ranges from a few percent to 100%. The larger and denser the initial mass, the greater chance that an unaffected nucleus will survive the flight. Otherwise we will only observe the splendid display of a fireball. As a general conclusion then to this section, we may state that the surviving iron meteorites range from 3 cm to 300 cm in diameter. Smaller ones are completely burned up or never recovered, and larger ones tend to be drastically reduced in size by cratering impact. In a following section, on page 49, we shall examine the effect of heating and ablation on the recovered material.

Sound Phenomena

Meteorite falls are always associated with sound phenomena. They are apparently of two entirely different kinds. The obvious one, which is always reported, is usually compared to the sound of a passing express train, an airplane, or simply rolling thunder. The other one is occasionally reported and described as hissing, comparable to the sound produced by frying bacon or plunging a heated iron in cold water. This sound is reported to occur *simultaneously* with the passing fireball, which may be 100 km distant; here we evidently meet the paradox of a sound propagating with the velocity of light.

A. The normal impressive sound phenomena arrive at an observer located near the impact point long after the fireball has been extinguished but usually before the meteorite has landed. Eyewitnesses to Avče, Bogou, N'Kandhla and Soroti thus are unanimous in having first heard the sonic booms and then seen the body impact near them approximately ½-2 minutes afterwards. In other cases, like Hraschina and Muzzaffarpur, it appears that the sounds had not yet ceased when the masses landed. The meteorites must evidently fall the last part of their journey with average velocities slightly below that of sound, as also discussed on page 30.

Eyewitnesses located further distant have reported that the sounds are heard from 30 seconds to 5 minutes after the fireball appearance, and that the sound train has a duration of 5 seconds to 3 minutes. The sounds are caused by the violent displacement of the air column along the whole trajectory. To a minor degree sound may be emitted when the meteorite bursts and individual fragments follow their own trajectories; the multiple sounds reported from multiple falls may be understood in this way. The sounds may be perceived up to at least 100 km from the projection of the trajectory on the surface of the earth, but local conditions may greatly influence the quality of the perception. In exceptional cases it has occurred that eyewitnesses less than a kilometer from the point of impact have heard absolutely nothing, while distant observers have reported the usual rumble and sonic booms.

The velocity of sound in gases c, is expressed by the Laplace formula (1843),

$$c^2 = \frac{C_p}{C_v} \cdot \frac{RT}{M},$$

where C_p is the heat capacity at constant pressure, C_v the heat capacity at constant volume, R is the gas constant, T the absolute temperature in degrees Kelvin and M the average molecular weight of the gas. For air it has been shown that the predicted classical sound velocity remains independent of atmospheric pressure to significant altitudes (at least 30 km); i.e., the overriding cause of sound velocity variation in still dry air is atmospheric temperature fluctuations. The velocity dependence on the temperature is

$$c_T = c_o \sqrt{T/273},$$

where c_0 is the velocity at 0° C, 331.5 m/sec.

The thermodynamic state of the atmosphere is non-uniform both vertically and horizontally. The sound wave from a penetrating meteorite will pass regions of varying temperature, and it will be refracted according to Snell's law $c_1/\sin i_1 = c_2/\sin i_2$. Moreover, wind velocity will influence the path of the sound wave. The wind velocity is vectorialy additive to the sound velocity; and since wind velocities in the high atmosphere range from 10 to 100 m/sec, their contribution is far from negligible; see Figure 13.

It is thus understandable that the local atmospheric conditions and the surface topography can to a large extent influence the propagation, refraction and attenuation of the sound from a passing meteorite. Within the limits of the acoustic field, both silent zones and zones where the sound phenomena are intensified have often been observed. In general, a casual observer will first hear the detonations from the lowest part of the trajectory and then gradually hear the rumble from the more and more distant parts of the trajectory. Witnesses who did not actually see the trajectory itself have therefore often concluded that the meteorite passed in the direction opposite to the real one, due to this confusing displacement of sounds.

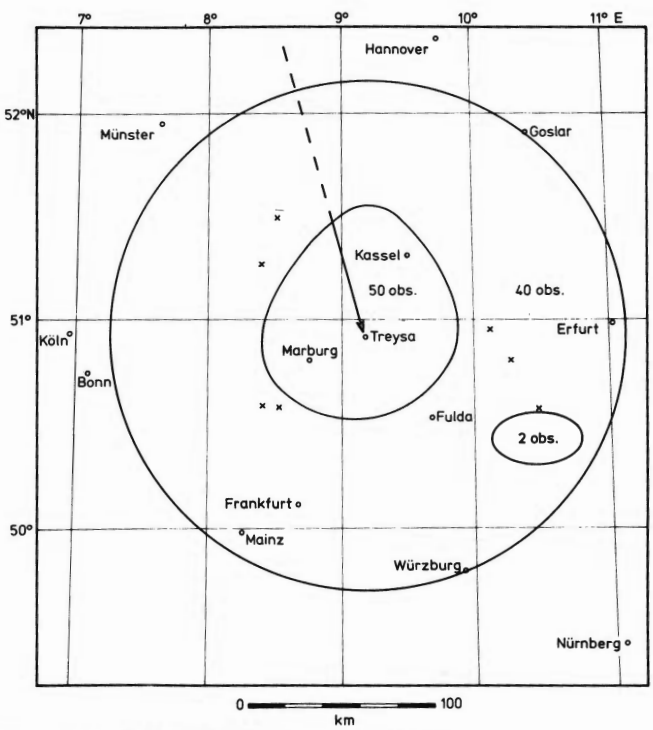

Figure 20A. The iron meteorite Treysa fell April 3, 1916 in Hesse, Germany. Within the two inner zones, 52 observers reported significant detonations. Within the large circle, 40 observers saw the large flash but heard nothing. Seven observers, marked with crosses, heard the peculiar hissing noises. (From Wegener 1917; and Lamar & Romig 1964)

B. People actively engaged in meteorite field work have again and again been confronted by witnesses who claim that hissing sounds were heard at the instant of the meteorite's flight. Nininger (1939e) suggested that the effects were caused by electromagnetic waves emitted from the fireball trajectory; under proper conditions these waves might, on meeting metallic structures on the Earth, be transformed into true sound waves. Astapovich (1951) has thoroughly examined a large number of cases and presented a catalog of the reports concerning both fireballs and meteorites. Most authors have, however, rejected these claims and explained them as subjective associations of sound and light phenomena. A close scrutiny of numerous independent reports leaves, however, little doubt that the sounds are real, and further that they are usually of high frequency and low intensity, so that not everybody is capable of hearing them. Animals, particularly dogs, have been alarmed by these sounds, as may be seen from the following report describing the occasion of the Beddgelert meteorite fall in 1949:

> The manager of the Hotel at Beddgelert was awakened .... by the barking of his dog – in itself an unusual occurrence. He was for the moment unable to account for the dog's behaviour, but realized after a few seconds that something extraordinary was happening when he heard a series of irregularly spaced bangs which he – being an ex-naval man – says sounded like a naval broadside (Chacket et al. 1950).

Later the same day he realized that his hotel roof had been penetrated by a 794 g stone meteorite, page 30.

Recently, Lamar & Romig (1964) have discussed the anomalous sounds and also accumulated several reports of other atmospheric disturbances which may have been caused by the rapid propagation of a weak electromagnetic field. They discuss various alternatives but seem to favor the idea that the sound is being caused by electric discharges on the ground. It is not known how the fireball could disturb the earth's electric field sufficiently to cause such discharges. It is possible that the ionized wake acts as a conductor and thus forms a channel from the D layer to lower altitudes. If the atmosphere is considered to be one plate of a condenser, such a channel might affect the earth's electric field sufficiently to cause a discharge.